# Atmospheric Chemistry of 1,3,5-Trioxane: UV Spectra of c-$C_3H_5O_3$(•) and (c-$C_3H_5O_3$)$O_2$(•) Radicals, Kinetics of the Reactions of (c-$C_3H_5O_3$)$O_2$(•) Radicals with NO and $NO_2$, and Atmospheric Fate of the Alkoxy Radical (c-$C_3H_5O_3$)O(•)

**J. Platz, L. K. Christensen, J. Sehested,*,† and O. J. Nielsen*,†**

*Atmospheric Chemistry, Plant Biology and Biogeochemistry Department, Risø National Laboratory, DK-4000, Roskilde, Denmark*

**T. J. Wallington*,‡**

*Ford Motor Company, 20000 Rotunda Drive, Mail Drop SRL-3083, Dearborn, Michigan 48121-2053*

**C. Sauer, Ian Barnes,*,§ and K. H. Becker**

*Bergische Universität Wuppertal, Physikalische Chemie-FB9, Gauss-Strasse 20, D-42097 Wuppertal, Germany*

**R. Vogt**

*Ford Forschungszentrum Aachen GmbH, Technologiezentrum am Europaplatz, Dennewartstrasse 25, D-52068 Aachen, Germany*

*Received: January 29, 1998; In Final Form: April 13, 1998*

A pulse radiolysis technique was used to measure the UV absorption spectra of c-$C_3H_5O_3$(•) and (c-$C_3H_5O_3$)-$O_2$(•) radicals over the range 220−300 nm, with $\sigma$(c-$C_3H_5O_3$(•))$_{250\ nm} = (5.2 \pm 0.7) \times 10^{-18}$ and $\sigma$((c-$C_3H_5O_3$)-$O_2$(•))$_{250\ nm} = (3.7 \pm 0.4) \times 10^{-18}$ cm$^2$ molecule$^{-1}$. The self-reaction rate constant for the c-$C_3H_5O_3$(•) radicals, defined as d[c-$C_3H_5O_3$(•)]/d$t = 2k_4$[c-$C_3H_5O_3$(•)]$^2$, was $k_4 = (3.1 \pm 0.6) \times 10^{-11}$ cm$^3$ molecule$^{-1}$ s$^{-1}$. The rate constants for reactions of (c-$C_3H_5O_3$)$O_2$(•) radicals with NO and $NO_2$ were $k_6 = (5.8 \pm 1.4) \times 10^{-12}$ and $k_7 = (1.1 \pm 0.2) \times 10^{-11}$ cm$^3$ molecule$^{-1}$ s$^{-1}$, respectively. The rate constants for the reaction of F atoms with 1,3,5-trioxane and the reaction of c-$C_3H_5O_3$(•) radicals with $O_2$ were $k_3 = (1.1 \pm 0.4) \times 10^{-10}$ and $k_2 = (7.4 \pm 1.1) \times 10^{-12}$ cm$^3$ molecule$^{-1}$ s$^{-1}$, respectively. Relative rate techniques were used to measure the rate constants for the reactions of OH radicals and Cl atoms with 1,3,5-trioxane and Cl atoms with H(O)-$COCH_2OC$(O)H, $k_{20} = (6.0 \pm 1.0) \times 10^{-12}$, $k_{24} = (1.0 \pm 0.2) \times 10^{-10}$, and $k_{25} = (5.1 \pm 1.0) \times 10^{-13}$ cm$^3$ molecule$^{-1}$ s$^{-1}$, respectively. FTIR−smog chamber systems were used to show that the atmospheric fate of the alkoxy radical (c-$C_3H_5O_3$)O(•) is decomposition via C−O bond scission leading to the formation of H(O)-$COCH_2OC$(O)H (methylene glycol diformate). The IR spectrum of the peroxynitrate (c-$C_3H_5O_3$)$O_2NO_2$ is presented. The results are discussed with respect to the atmospheric chemistry of 1,3,5-trioxane.

## 1. Introduction

Ethers are an important class of automotive fuel additives. For example, methyl *tert*-butyl ether (MTBE), ethyl *tert*-butyl ether (ETBE), *tert*-amyl methyl ether (TAME), and diisopropyl ether (DIPE) are widely used octane enhancing additives in gasoline. In addition, ethers such as dimethyl ether,[1] and dimethoxymethane are under consideration as alternative diesel fuels. To predict the environmental impact of ether fuels and fuel additives it is desirable to understand how the structure of such molecules impacts their atmospheric reactivity and degradation pathways. 1,3,5-Trioxane is not used currently as an automotive fuel additive but is a convenient model compound whose chemistry provides insight into the behavior of alkyl peroxy, and alkoxy radicals connected directly to two oxygen ether linkages. As part of a collaborative study of the atmospheric chemistry of automotive fuel additives, we have conducted an investigation of the atmospheric chemistry of 1,3,5-trioxane.

The atmospheric degradation of 1,3,5-trioxane is initiated by reaction with OH radicals giving an alkyl radical which adds $O_2$ to form an alkylperoxy radical:

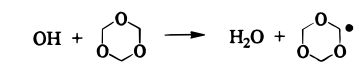


(1)

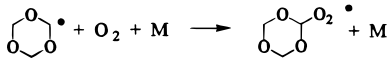


(2)

We have used pulse radiolysis coupled with time-resolved UV−vis absorption spectroscopy to determine the UV absorption spectra of the alkyl and alkyl peroxy radicals derived from 1,3,5-trioxane and the kinetics of reactions 2−4, 6, and 7.

FTIR product studies were performed to determine the fate of the alkoxy radical (c-$C_3H_5O_3$)O(•) formed in reaction 6a.

† E-mail: jens.sehested@risoe.dk.
‡ E-mail: twalling@ford.com.
§ E-mail: barnes@physchem.uni-wuppertal.de.

S1089-5639(98)00954-2 CCC: $15.00 
Published on Web 06/02/1998

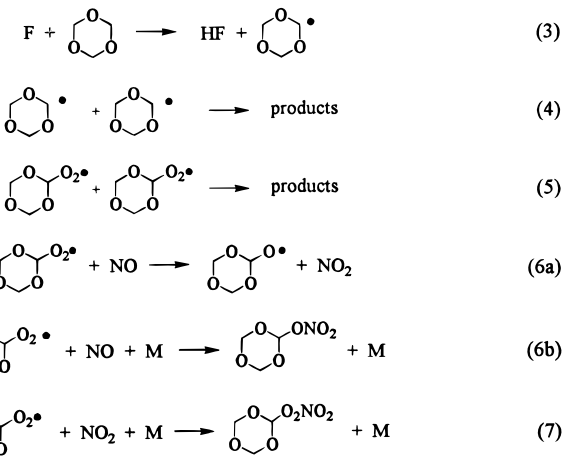


(3) (4) (5) (6a) (6b) (7)

## 2. Experimental Section

The three experimental systems used are described elsewhere[2−4] and are discussed briefly here.

**2.1. Pulse Radiolysis System.** c-$C_3H_5O_3$(•) radicals were generated from 1,3,5-trioxane by the pulsed radiolysis of $SF_6$/c-$C_3H_6O_3$ gas mixtures in a 1 L stainless steel reaction cell with a 30 ns pulse of 2 MeV electrons from a Febetron 705 field emission accelerator. $SF_6$ was always in great excess and was used to generate fluorine atoms:

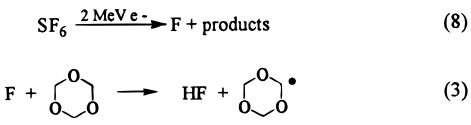


(8) (3)

The radiolysis dose was varied by insertion of stainless steel attenuators between the accelerator and the reaction cell. In this work we refer to the radiolysis dose as a fraction of the maximum dose that is achievable. The fluorine atom yield was calibrated by monitoring the transient absorption at 260 nm by $CH_3O_2$ radicals produced by pulse radiolysis of $SF_6/CH_4/O_2$ mixtures, as described previously.[5] Using $\sigma(CH_3O_2) = 3.18 \times 10^{-18}$ cm$^2$ molecule$^{-1}$,[6] the F atom yield was determined to be $(3.16 \pm 0.35) \times 10^{15}$ molecules cm$^{-3}$ at full radiolysis dose and 1000 mbar of $SF_6$.[5] The quoted error includes 10% uncertainty in $\sigma(CH_3O_2)$ and two standard deviations from the experimental absorption measurements. Unless otherwise stated, all uncertainties reported in this paper are two standard deviations and standard error propagation methods were used.

The analysis light was provided by a pulsed 150 W xenon arc lamp and was multipassed through the reaction cell using internal White cell optics to give total optical path lengths of 80 or 120 cm. After leaving the cell, the light was guided through a monochromator and detected by a photomultiplier (to record absorption transients) or by a diode array (to record absorption spectra). All absorption transients were derived from single pulse experiments. Using the photomultiplier detector the spectral resolution was 0.8 nm while it was 1 nm when the diode array was used to record spectra. Spectral calibration was achieved using a Hg pen ray lamp.

Reagent concentrations used were the following: $SF_6$, 948−997 mbar; 1,3,5-trioxane, 3 mbar; $O_2$, 0.3−40.0 mbar; $CH_4$, 1.2−49.0; $NO_2$, 0.23−1.18 mbar; NO, 0.32−1.02 mbar. All experiments were performed at 296 K and 1000 mbar total pressure. Chemicals were supplied by the following: $SF_6$ (99.9%), Gerling and Holz; 1,3,5-trioxane (>99%), Fluka Chemica; $O_2$, (ultrahigh purity), L'Air Liquide; $CH_4$ (>99.95%), L'Air Liquide; $NO_2$ (>98%), Linde Technische Gase; NO (99.8%), Messer Griesheim. All chemicals were used as received.

Six sets of experiments were performed using the pulse radiolysis system. First, the rate constant for reaction of F atoms with 1,3,5-trioxane was determined using the pulse radiolysis of $SF_6$/1,3,5-trioxane/$CH_4$ mixtures. Second, the UV absorption spectra of the alkyl and alkyl peroxy radicals derived from 1,3,5-trioxane were obtained by using the diode array camera to capture the UV absorption following radiolysis of $SF_6$/1,3,5-trioxane and $SF_6$/1,3,5-trioxane/$O_2$ mixtures. Third, the rate constant for reaction 4 was determined from the rate of the decay of the absorption at 250 nm, following the radiolysis of $SF_6$/1,3,5-trioxane. Fourth, the rate constant for the association reaction between $O_2$ and the alkyl radical derived from 1,3,5-trioxane was measured by monitoring the loss of alkyl radicals in the presence of $O_2$. Fifth, the rate of $NO_2$ formation following radiolysis of $SF_6$/1,3,5-trioxane/$O_2$/NO mixtures was used to measure the rate constant for the reaction between NO and the peroxy radical derived from 1,3,5-trioxane, $k_6$. Sixth, $k_7$ was determined by monitoring the rate of $NO_2$ loss following radiolysis of $SF_6$/1,3,5-trioxane/$O_2$/$NO_2$ mixtures (eqs 6a,b and 7).

**2.2. FTIR−Smog Chamber Systems.** FTIR−smog chamber systems at Wuppertal and Ford were used to investigate the kinetics of the reactions of OH radicals and Cl atoms with 1,3,5-trioxane and the atmospheric fate of the alkoxy radical (c-$C_3H_5O_3$)O(•). In Wuppertal the experiments were performed using a 405 L Pyrex reactor[7] and a 1080 L quartz reactor.[8] The 405 L reactor is surrounded by 18 super actinic fluorescent lamps (Philips TL05/40 W: $320 < \lambda < 480$ nm, $\lambda_{max} = 360$ nm). UV radiation for experiments conducted in the 1080 L quartz reaction chamber was provided by either 32 low-pressure mercury lamps ($\lambda_{max} = 254$ nm) or 32 superactinic fluorescent lamps. At Ford the experiments were performed using a 140 L Pyrex reactor[9] surrounded by 22 fluorescent blacklamps (GTE F40BLB, $\lambda > 300$ nm). FTIR systems are interfaced to the reactors. Loss of reactants and the formation of products were monitored in situ by FTIR spectroscopy, using a resolution of 0.25, 1, and 1 cm$^{-1}$ and analyzing path lengths of 27, 50, and 485 m for the 140, 405, and 1080 L reactors, respectively.

All experiments were performed at 700−750 Torr total pressure ($N_2 + O_2$) and $296 \pm 3$ K. The photolysis of $Cl_2$ was used as the Cl atom radical source. OH radicals were generated by either the 254 nm photolysis of $H_2O_2$ or the UV irradiation ($\lambda > 300$ nm) of $CH_3ONO$/NO mixtures.

## 3. Results and Discussion

**3.1. Reaction of F Atoms with 1,3,5-Trioxane.** To measure $k_3$, experiments were performed in which the observed maximum transient absorbance at 260 nm was measured following the radiolysis of $SF_6$/1,3,5-trioxane/$CH_4$ mixtures. The radiolysis dose (41.6% of full dose) and total pressure (1000 mbar) were held fixed. The concentrations of 1,3,5-trioxane and $CH_4$ were varied over the ranges 0−3.2 mbar and 0−48.1 mbar, respectively. Figure 1 shows the observed maximum absorbance as a function of the concentration ratio [$CH_4$]/1,3,5-trioxane. Reactions 3 and 9 compete for the available F atoms.

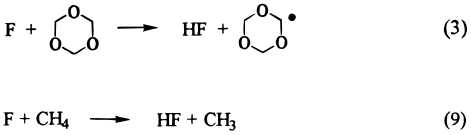


(3) (9)

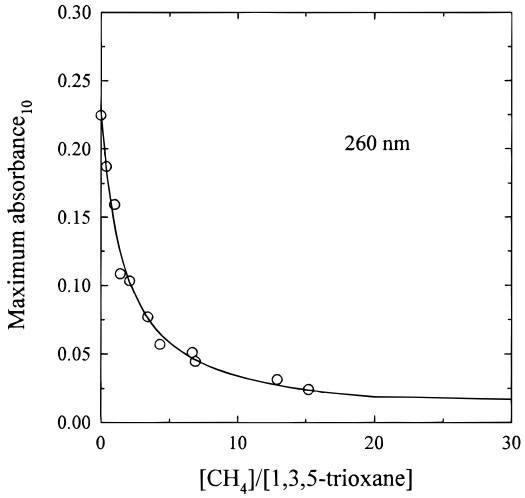


**Figure 1.** Plot of the maximum absorbance observed at 260 nm following the radiolysis of 1,3,5-trioxane/$CH_4$/$SF_6$ mixtures versus the concentration ratio [$CH_4$]/1,3,5-trioxane.

$CH_3$ radicals do not absorb significantly at 260 nm. In contrast the alkyl radicals derived from 1,3,5-trioxane absorb appreciable at 260 nm (see section 3.3). As shown in Figure 1, as the concentration ratio [$CH_4$]/1,3,5-trioxane increases, the maximum absorbance decreases because a greater fraction of the F atoms react with $CH_4$ to give $CH_3$ radicals. The solid line in Figure 1 is a three parameter fit of the following expression to the experimental data:

$$A_{max} = (A_R + A_{CH_3}(k_9/k_3)[CH_4]/1,3,5\text{-trioxane})/ (1 + (k_9/k_3)[CH_4]/1,3,5\text{-trioxane})$$

Here $A_{max}$ is the observed maximum absorbance, $A_R$ is the maximum absorbance of alkyl radicals expected if only alkyl radicals from 1,3,5-trioxane were produced, and $A_{CH_3}$ is the maximum absorbance expected if only $CH_3$ radicals were produced. $A_R$ and $A_{CH_3}$ were measured to have an absorbance of 0.225 and 0.014, respectively. The parameters $A_R$, $A_{CH_3}$ and $k_9/k_3$ were varied simultaneously; the best fit was obtained with $A_R = (0.23 \pm 0.02)$, $A_{CH_3} = (2.0 \pm 16.4) \times 10^{-3}$, and $k_9/k_3 = (0.60 \pm 0.19)$. Using $k_9 = (6.8 \pm 1.4) \times 10^{-11}$ [10] gives $k_3 = (1.1 \pm 0.4) \times 10^{-10}$ cm$^3$ molecule$^{-1}$ s$^{-1}$.

**3.2. Spectrum of Alkyl Radicals Derived from 1,3,5-Trioxane.** Following the pulse radiolysis of $SF_6$/1,3,5-trioxane mixtures, a rapid (complete within 0.5−1.5 $\mu$s) increase in absorption was observed at 250 nm, followed by a slower decay. Figure 2A shows the transient absorption at 250 nm following the radiolysis of a mixture of 997 mbar $SF_6$ and 3 mbar 1,3,5-trioxane. No absorption was observed when either 997 mbar of $SF_6$ or 3 mbar of 1,3,5-trioxane was radiolyzed separately. We ascribe the absorption shown in Figure 2A to the formation of alkyl radicals and their subsequent loss by self-reaction. As with all reactions of F atoms with saturated organic compounds, it is expected that reaction 3 proceeds via H-atom abstraction to give alkyl radicals. To work under conditions where 100% of the F atoms are converted into alkyl radicals, it is necessary to consider potential interfering radical−radical reactions such as (4) and (10). To check for such complications, experiments

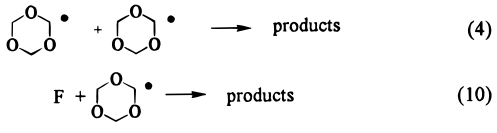


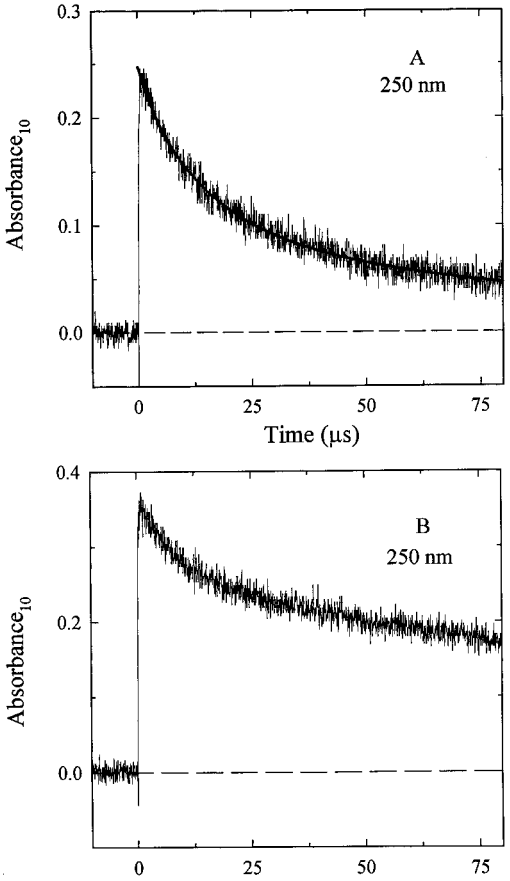


**Figure 2.** (A) Transient absorbance at 250 nm following the pulsed radiolysis (dose = 42% of maximum) of a mixture of 3 mbar 1,3,5-trioxane and 997 mbar $SF_6$. The UV path length was 80 cm. A second-order decay fit to the experimental data is shown. (B) Transient absorbance at 250 nm following the pulsed radiolysis (maximum dose) of a mixture of 3 mbar 1,3,5-trioxane, 40 mbar $O_2$, and 977 mbar $SF_6$. The UV path length was 80 cm.

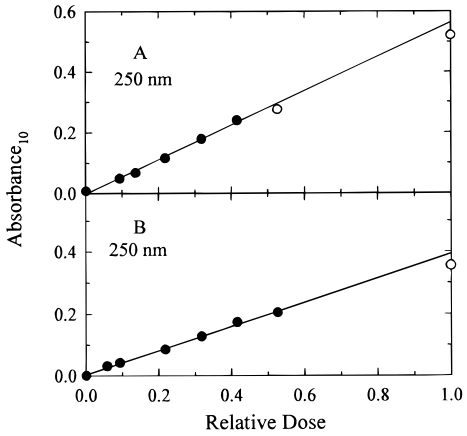


**Figure 3.** (A) Maximum transient absorbance at 250 nm following the pulsed radiolysis of mixtures of 3 mbar 1,3,5-trioxane and 997 mbar $SF_6$ versus the radiolysis dose. The UV path length was 120 cm. (B) Maximum transient absorbance at 250 nm following the pulsed radiolysis of mixtures of 3 mbar 1,3,5-trioxane, 40 mbar $O_2$, and 957 mbar $SF_6$ versus the radiolysis dose. The UV path length was 120 cm. The solid lines in A and B are linear regressions of the low-dose data (filled circles).

were performed using mixtures of 997 mbar of $SF_6$ and 3 mbar of 1,3,5-trioxane, with the maximum transient absorption at 250 nm measured as a function of radiolysis dose. Figure 3A shows the observed maximum absorbance as a function of the dose. As seen from Figure 3A, the absorption observed in experiments

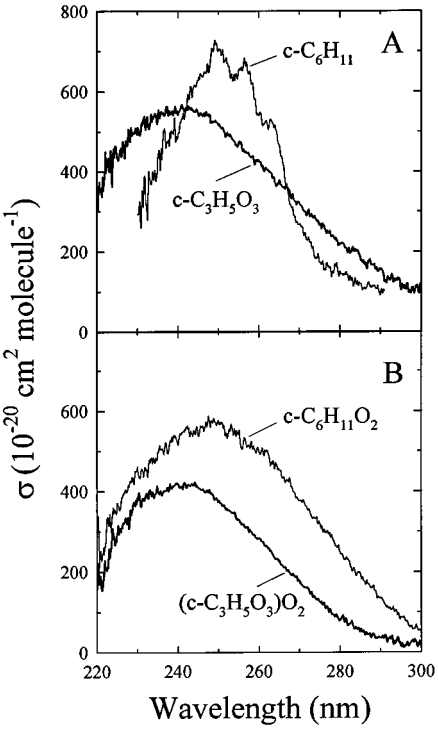


**Figure 4.** (A) UV-absorption spectra of the alkyl radicals derived from 1,3,5-trioxane and cyclohexane. (B) UV-absorption spectra of the peroxy radicals derived from 1,3,5-trioxane and cyclohexane.[11]

**TABLE 1: Absorption Cross Sections Measured in This Work**

| wavelength (nm) | $\sigma$(c-$C_3H_5O_3$(•)) ($10^{-20}$ cm$^2$ molecule$^{-1}$) | $\sigma$((c-$C_3H_5O_3$)$O_2$(•)) ($10^{-20}$ cm$^2$ molecule$^{-1}$) |
|---|---|---|
| 220 | 336 | 180 |
| 230 | 502 | 377 |
| 240 | 546 | 418 |
| 250 | 518 | 372 |
| 260 | 427 | 283 |
| 270 | 423 | 177 |
| 280 | 218 | 79 |
| 290 | 156 | 36 |
| 300 | 114 | 20 |

using maximum dose was significantly less than that expected on the basis of a linear extrapolation of the low-dose data. This observation suggests that unwanted radical−radical reactions such as reactions 4 and 10 become important at high radical concentrations.

The line through the experimental data in Figure 3A is a linear least-squares fit to the low-dose data and has a slope of 0.567 ± 0.043. Combining this slope with the F atom yield of (3.16 ± 0.35) × $10^{15}$ molecules cm$^{-3}$ (full dose and [$SF_6$] = 1000 mbar), we obtain $\sigma_{250\ nm}$(alkyl) = (5.18 ± 0.70) × $10^{-18}$ cm$^2$ molecule$^{-1}$. The quoted error includes statistical and potential systematic uncertainties associated with calibration of the F atom yield (see section 2.1)

The spectrum of the alkyl radical was measured by recording the initial absorbance following the pulsed radiolysis of $SF_6$/1,3,5-trioxane mixtures using a diode array. The delay was 1 $\mu$s, the integration time was 10 $\mu$s, and the spectral resolution was 1 nm. The initial absorbances were scaled to that at 250 nm and placed upon an absolute basis using $\sigma_{250\ nm}$ = 5.18 × $10^{-18}$ cm$^2$ molecule$^{-1}$. The results are given in Table 1 and Figure 4A. For comparison the UV absorption spectrum of the cyclohexyl radical is also given in Figure 4A.[11] The UV spectrum of the alkyl radical derived from 1,3,5-trioxane has a lower maximum and is blue shifted by approximately 10 nm compared to the UV absorption spectrum of cyclohexyl radical.

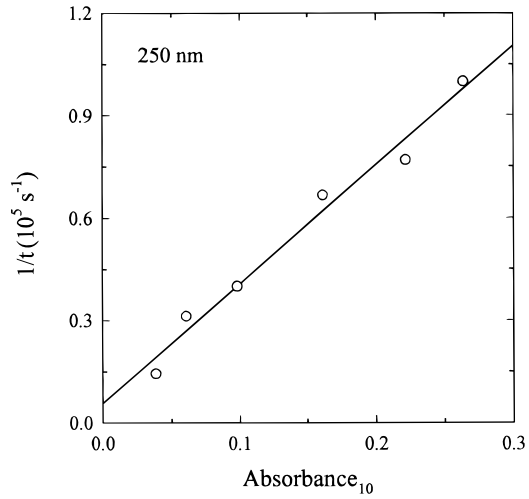


**Figure 5.** Plot of the reciprocal half-life for self-reaction of c-$C_3H_5O_3$-(•) radicals as a function of the maximum absorbance at 250 nm.

**3.3. Kinetic Study of the Self-Reaction of c-$C_3H_5O_3$(•) Radicals.** Figure 2A shows a typical absorption trace obtained by pulse radiolysis of a mixture of 997 mbar $SF_6$ and 3 mbar 1,3,5-trioxane. The trace shows a rapid increase in absorption at 250 nm followed by a slower decay. We ascribe the decay to the self-reaction of the alkyl radical, via reaction 4. The decay was fitted with the second-order decay expression $A(t) = (A_0 - A_{inf})/(1 + 2k_4(A_0 - A_{inf})t) + A_{inf}$, where $A(t)$ is the measured absorbance at time $t$, $A_0$ and $A_{inf}$ are the absorbances extrapolated to time zero and infinite time, respectively. The fit is shown in Figure 2A. No residual absorption was observed, indicating the absence of any long-lived products which absorb significantly at 250 nm.

The reciprocal half-lives, $1/t_{1/2}$ (derived from the fits), are plotted as a function of $A_0$ in Figure 5. The alkyl radical concentration was varied by varying the initial F atom concentration. A linear least-squares fit of the data in Figure 5 gives a slope of (3.49 ± 0.51) × $10^5$ s$^{-1}$ = ($k_4$ × 2 ln 10)/($\sigma$(alkyl)L), where $\sigma$(alkyl) is the absorption cross section of the c-$C_3H_5O_3$-(•) radical and L is the optical path length (80 cm). The intercept of the linear regression of the data, (0.06 ± 0.08) × $10^5$ s$^{-1}$, is not significantly different from zero. The slope of (3.49 ± 0.51) × $10^5$ s$^{-1}$ can be combined with $\sigma_{250\ nm}$(c-$C_3H_5O_3$(•)) = (5.18 ± 0.70) × $10^{-18}$ cm$^2$ molecule$^{-1}$ to give $k_4$ = (3.1 ± 0.6) × $10^{-11}$ cm$^3$ molecule$^{-1}$ s$^{-1}$. The quoted error includes statistical uncertainties associated with both the slope in Figure 5 and $\sigma_{250\ nm}$(c-$C_3H_5O_3$(•)). $k_4$ is similar to the rate constant for the self-reaction of alkyl radicals derived from 1,4-dioxane, (3.3 ± 0.4) × $10^{-11}$ cm$^3$ molecule$^{-1}$ s$^{-1}$.[12]

**3.4. Association Reaction between $O_2$ and c-$C_3H_5O_3$(•) Radicals.** The kinetics of reaction 2 were studied by monitoring the loss of c-$C_3H_5O_3$(•) radicals in the presence of $O_2$. As seen from Figure 4, both the alkyl, c-$C_3H_5O_3$(•), and alkyl peroxy radical, (c-$C_3H_5O_3$)$O_2$(•), absorb significantly in the UV. Fortunately, the absorption by the alkyl radical is greater than that of the peroxy radical and so the conversion of alkyl into peroxy radical can be observed by monitoring the decrease in absorption during the reaction. A monitoring wavelength of 290 nm was selected on the basis of the low noise of the optical system and significant difference in the absorption cross sections of the alkyl and alkyl peroxy radicals at this wavelength.

Reaction mixtures of 497 or 997 mbar of $SF_6$, 3.0 mbar of 1,3,5-trioxane, and 0.29−2.30 mbar of $O_2$ were employed. From

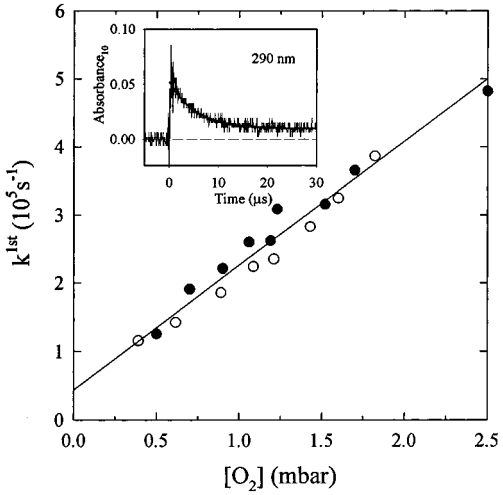


**Figure 6.** Pseudo first-order rate constants for the formation of (c-$C_3H_5O_3$)$O_2$(•) radicals as a function of the $O_2$ concentration in 500 (○) and 1000 (●) mbar of $SF_6$, diluent. The insert shows an experimental transient obtained using a mixture of 3 mbar 1,3,5-trioxane and 0.86 mbar of $O_2$, in 996 mbar of $SF_6$. The UV path length was 80 cm, and the radiolysis dose was 42% of maximum. The smooth curve in the insert is the first-order decay fit.

$k_3 = 1.1 \times 10^{-10}$ cm$^3$ molecule$^{-1}$ s$^{-1}$ it follows that in the presence of 3 mbar of 1,3,5-trioxane the lifetime of F atoms with respect to conversion into c-$C_3H_5O_3$(•) radicals is 0.12 $\mu$s. Assuming that c-$C_3H_5O_3$(•) radicals behave like other alkyl radicals and add $O_2$ with a rate constant of the order $10^{-12}$–$10^{-11}$ cm$^3$ molecule$^{-1}$ s$^{-1}$, the lifetime of c-$C_3H_5O_3$(•) radicals with respect to conversion into (c-$C_3H_5O_3$)$O_2$(•) radicals will be of the order of 1 $\mu$s. Consistent with expectations, the pulsed radiolysis of $SF_6$/1,3,5-trioxane/$O_2$ mixtures produced absorption transients which consisted of a initial rapid increase in absorption (complete within 0.2 $\mu$s) and then a rapid decay which occurred on a time scale of 1−10 $\mu$s and followed first-order kinetics. The insert in Figure 6 shows a typical absorption transient together with a first-order fit. As seen from Figure 6, the pseudo-first-order rate, $k^{1st}$, increased linearly with the $O_2$ concentration. It seems reasonable to ascribe the decay of absorption to loss of c-$C_3H_5O_3$(•) radicals via reaction with $O_2$. Experiments were performed in the presence of either 500 or 1000 mbar of $SF_6$ diluent. As seen from Figure 6, there was no discernible effect of total pressure suggesting that reaction 2 is at, or near, the high-pressure limit in 500−1000 mbar of $SF_6$. This behavior is consistent with the available database for the addition of $O_2$ to large ($\geq C_3$) alkyl radicals.[13] Linear least-squares analysis of the data in Figure 6 gives $k_2 = (7.4 \pm 1.1) \times 10^{-12}$ cm$^3$ molecule$^{-1}$ s$^{-1}$. This value is similar to the rate constant of $(8.8 \pm 0.9) \times 10^{-12}$ cm$^3$ molecule$^{-1}$ s$^{-1}$ for the reaction between (c-$C_4H_7O_2$)$O_2$(•) radicals and $O_2$. The *y*-axis intercept is $(0.44 \pm 0.24) \times 10^5$ s$^{-1}$ and is ascribed to a small but nonnegligible contribution of the self-reaction to loss of the alkyl radicals.

**3.5. Spectrum of Alkyl Peroxy Radicals Derived from 1,3,5-Trioxane.** Following the pulse radiolysis of mixtures of 957 mbar $SF_6$, 3 mbar 1,3,5-trioxane, and 40 mbar $O_2$, a rapid increase (complete within 0.5−2.0 $\mu$s) in the UV absorbance was observed, followed by a slower decay. An example is shown in Figure 2B. We ascribe this UV absorbance to the formation of the peroxy radical via reaction 2. To work under conditions where a known fractions of the F atoms are converted into alkyl peroxy radicals, it is necessary to consider potential interfering secondary chemistry. Potential complications include unwanted radical−radical reactions such as reactions 4 and 10−12 and loss of F atoms by reaction with molecular oxygen, reaction 13.

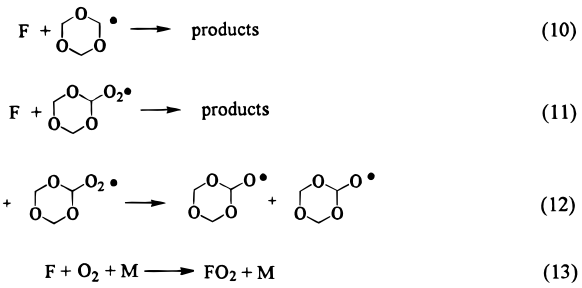


In section 3.1 we report $k_3 = (1.1 \pm 0.4) \times 10^{-10}$ cm$^3$ molecule$^{-1}$ s$^{-1}$. Using $k_{l3} = (1.9 \pm 0.3) \times 10^{-13}$ cm$^3$ molecule$^{-1}$ s$^{-1}$,[14] we calculate that 2.3% of the F atoms are converted into $FO_2$ radicals and 97.7% into alkyl peroxy radicals. Corrections were computed for the presence of $FO_2$ radicals using literature data for the UV spectrum of $FO_2$ radicals.[15] The corrections were <11.5% (highest at 220 nm).

There are no literature data concerning the kinetics of reactions 10−12; hence, we cannot calculate their importance. To check for these unwanted radical−radical reactions, the transient absorbance at 250 nm was measured using mixtures of 957 mbar $SF_6$, 3 mbar 1,3,5-trioxane, and 40 mbar $O_2$ with the radiolysis dose varied by 1 order of magnitude. The UV path length was 80 cm. Figure 3B shows the observed maximum absorbance of the experimental transients at 250 nm as a function of dose. As seen from Figure 3B, in experiments employing doses of 0.5 or greater the transient absorbance falls below that expected from a linear extrapolation of the low-dose data. We ascribe this to incomplete conversion of F atoms into alkyl peroxy radicals caused by secondary radical−radical reactions 4 and 10−12 at high radical concentrations. The solid line drawn through the data in Figure 3B is a linear least-squares fit of the low-dose data. The slope is 0.39 ± 0.02. From this value and the yield of F atoms of $(3.16 \pm 0.35) \times 10^{15}$ molecule cm$^{-3}$ (full dose and [$SF_6$] = 1000 mbar) we derive $\sigma$(250 nm) = $(3.72 \pm 0.42) \times 10^{-18}$ cm$^2$ molecule$^{-1}$. The quoted uncertainty includes both statistical and potential systematic uncertainties and so reflects the accuracy of the measurement.

To map out the spectrum of the alkyl peroxy radical, the maximum transient absorbance between 220 and 300 nm following the pulsed radiolysis of $SF_6$/1,3,5-trioxane/$O_2$ mixtures was recorded using a diode array. The delay was 5 $\mu$s, the integration time was 10 $\mu$s, and the spectral resolution was 1 nm. The initial absorbances were scaled to that at 250 nm and placed on an absolute basis using $\sigma(250\text{ nm}) = 3.72 \times 10^{-18}$ cm$^2$ molecule$^{-1}$. Results are given in Table 1 and Figure 4B. For comparison the UV spectrum of the cyclohexyl peroxy radical is also given in Figure 4B.[11] The UV absorption spectra of alkyl peroxy radicals typically consist of a broad featureless band in the region 200−300 nm with a maximum absorption cross section at ≈240−250 nm of $(4-5) \times 10^{-18}$ cm$^2$ molecule$^{-1}$.[16] Inspection of Figure 4B shows that the UV spectra of the peroxy radicals derived from 1,3,5-trioxane and cyclohexane are typical for this class of radical species.

**3.6. Kinetics of the Reaction between (c-$C_3H_5O_3$)$O_2$(•) Radicals and NO.** To study the kinetics of the reaction between NO and the alkyl peroxy radical derived from 1,3,5-trioxane, the rate of $NO_2$ formation was measured following the pulse radiolysis of 1,3,5-trioxane/$O_2$/NO/$SF_6$ mixtures. The initial conditions were 3 mbar 1,3,5-trioxane, 20 mbar $O_2$, and 0.32−

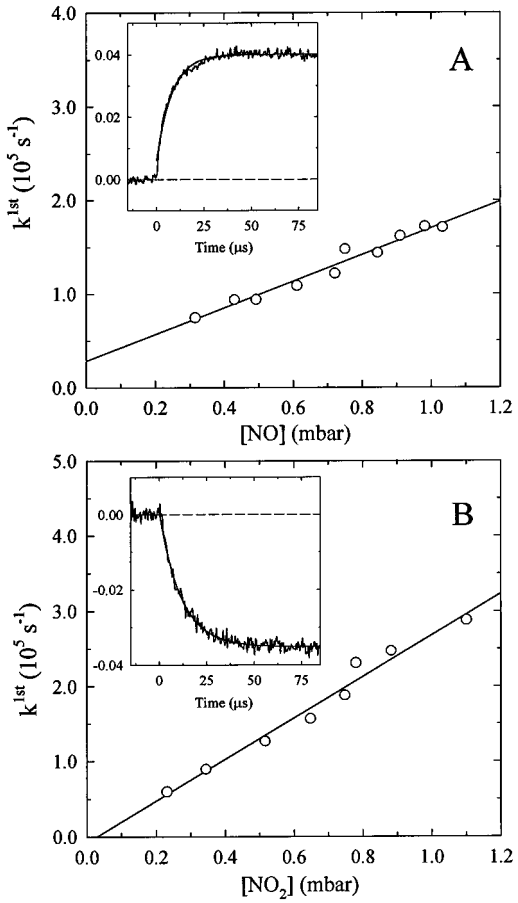


**Figure 7.** (A) Pseudo-first-order rate constants for formation of $NO_2$ following pulsed radiolysis of $SF_6$/1,3,5-trioxane/$O_2$/NO mixtures versus [NO]. The insert shows the transient absorbance at 400 nm observed following pulsed radiolysis (dose = 42% of maximum) of a mixture of 0.72 mbar NO, 3 mbar 1,3,5-trioxane, 20 mbar $O_2$, and 977 mbar $SF_6$. (B) Pseudo-first-order rate constants for decay of $NO_2$ following pulsed radiolysis of $SF_6$/1,3,5-trioxane/$O_2$/$NO_2$ mixtures versus [$NO_2$]. The insert shows the transient absorbance at 400 nm observed following pulsed radiolysis (dose = 22% of maximum) of a mixture of 0.344 mbar $NO_2$, 3 mbar 1,3,5-trioxane, 20 mbar $O_2$, and 977 mbar $SF_6$.

1.03 mbar NO, in 1000 mbar of $SF_6$ diluent. $NO_2$ was monitored using its absorbance at 400 nm. The insert in Figure 7A shows the absorbance as a function of time after the pulsed radiolysis of a mixture containing 0.72 mbar of NO. $NO_2$ absorbs strongly at 400 nm, and we ascribe the increased absorbance in the insert (Figure 7A) to $NO_2$ formation via reaction 6a. The absorption transients were fitted using a first-order kinetic expression, and resulting pseudo-first-order rate constants are plotted versus the initial NO concentration in Figure 7A. The expression used was $A(t) = ((A_{inf} - A_0)(1 - \exp(-k^{first}t)) + A_0$, where $A(t)$ is the time dependence absorbance, $A_{inf}$ is the extrapolated absorbance at infinite time, and $A_0$ is the extrapolated absorbance at $t = 0$. This method of measuring the kinetics of the reactions of alkyl peroxy radicals with NO has been used previously in our laboratory and is discussed in detail elsewhere.[17] As seen from Figure 7A, the pseudo-first-order rate constants, $k^{1st}$, increased linearly with the NO concentration. Linear least-squares analysis of the data in Figure 7A gives $k_6 = (5.8 \pm 0.8) \times 10^{-12}$ cm$^3$ molecule$^{-1}$ s$^{-1}$. The $y$-axis intercept is $(2.8 \pm 1.5) \times 10^4$ s$^{-1}$ and suggests that radical reactions such as the self-reaction, reaction 5, may contribute to the loss of the (c-$C_3H_5O_3$)$O_2$(•) radicals. The $NO_2$ yield calculated from the observed maximum absorbance was 79−100% of that expected if all F atoms were converted into peroxy radicals and all the peroxy radicals reacted via reaction 6a and is consistent with a small secondary loss of peroxy radicals and/or a minor contribution via reaction channel (6b). In light of the positive intercept in Figure 7A we choose to add an extra 10% uncertainty to $k_6$ resulting in a final value of $k_6 = (5.8 \pm 1.4) \times 10^{-12}$ cm$^3$ molecule$^{-1}$ s$^{-1}$.

**3.7. Kinetics of the Reaction between (c-$C_3H_5O_3$)$O_2$(•) Radicals and $NO_2$.** The kinetics of reaction 7 were studied by monitoring the decrease in absorbance at 400 nm following the pulsed radiolysis of mixtures of 3 mbar 1,3,5-trioxane, 20 mbar $O_2$, 0.231−1.100 mbar $NO_2$, and $SF_6$ added to 1000 mbar total pressure. The insert in Figure 7B shows the absorbance as a function of time after the radiolysis of a mixture containing 0.344 mbar of $NO_2$. The rate of decay of the absorbance at 400 nm increased linearly with the $NO_2$ concentration. It seems reasonable to ascribe the loss of absorbance to loss of $NO_2$ in the system. Three reactions could be responsible for the $NO_2$ loss:

$$F + NO_2 + M \longrightarrow FNO_2/FONO + M \quad (14)$$

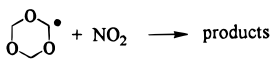

(15)

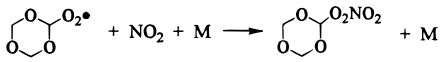

(7)

However, the time scale of the decay shown in the insert (Figure 7B) is only consistent with reaction 7 causing the loss of $NO_2$ (the lifetimes for both F atoms and c-$C_3H_5O_3$(•) radicals are $<0.4$ $\mu$s; see sections 3.1 and 3.4).

The smooth curve in the insert (Figure 7B) is the first-order fit which gives a pseudo-first-order rate constant, $k^{1st}$, = 8.96 $\times 10^4$ s$^{-1}$. To allow sufficient time for conversion of F atoms into the alkyl peroxy radicals the analysis of the decay traces was performed starting 2 $\mu$s after the radiolysis pulse. $k^{1st}$ values for eight experiments with different concentrations of $NO_2$ are shown in Figure 7B. Linear least-squares analysis of the data in Figure 7B gives a slope of $(2.76 \pm 0.36) \times 10^5$ s$^{-1}$ mbar$^{-1}$ which gives $k_7 = (1.1 \pm 0.2) \times 10^{-11}$ cm$^3$ molecule$^{-1}$ s$^{-1}$. The $y$-axis intercept in Figure 7B is $(-0.75 \pm 2.58) \times 10^4$ s$^{-1}$ and is not statistically significant.

**3.8. Kinetics of the Reaction of OH Radicals with 1,3,5-Trioxane.** The FTIR systems at Wuppertal and Ford were used to investigate the kinetics of the reaction of OH radicals with 1,3,5-trioxane. The techniques used are described elsewhere.[18] Photolysis of methyl nitrite or $H_2O_2$ was used as a source of OH radicals.

$$CH_3ONO \xrightarrow{h\nu} CH_3O + NO \quad (16)$$

$$CH_3O + O_2 \longrightarrow HCHO + HO_2 \quad (17)$$

$$HO_2 + NO \longrightarrow OH + NO_2 \quad (18)$$

$$H_2O_2 \xrightarrow{h\nu} 2\,OH \quad (19)$$

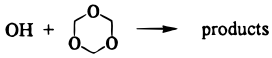

(20)

The kinetics of reaction 20 were measured relative to reactions 21 and 22.

$$OH + C_2H_4 \longrightarrow \text{products} \quad (21)$$

$$OH + \text{c-}C_6H_{12} \longrightarrow \text{products} \quad (22)$$

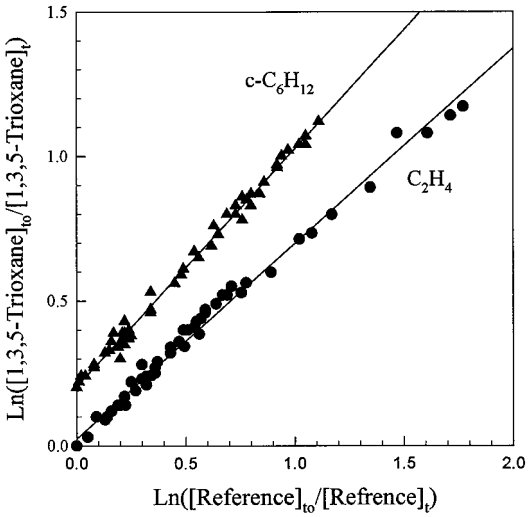


**Figure 8.** Decay of 1,3,5-trioxane versus $C_2H_4$ and cyclohexane when mixtures of these compounds were exposed to OH radicals. For clarity, the data using cyclohexane reference have been shifted vertically by 0.2 units.

The observed loss of 1,3,5-trioxane versus that of the reference compounds following the UV irradiation of mixtures of 0.5−4 mTorr of 1,3,5-trioxane, 1−5 mTorr of $C_2H_4$ or 0.4−1.0 mTorr of c-$C_6H_{12}$, and 100 mTorr of $CH_3ONO$ or 4−8 mTorr of $H_2O_2$ in 700−750 Torr total pressure of air is shown in Figure 8. Linear least-squares analysis gives $k_{20}/k_{21} = 0.67 \pm 0.05$ and $k_{20}/k_{22} = 0.82 \pm 0.04$. Using $k_{21} = 8.5 \times 10^{-12}$ [19] and $k_{22} = 7.5 \times 10^{-12}$ [19] gives $k_{20} = (5.7 \pm 0.4) \times 10^{-12}$ and $(6.2 \pm 0.3) \times 10^{-12}$ cm$^3$ molecule$^{-1}$ s$^{-1}$. We estimate that potential systematic errors associated with uncertainties in the reference rate constant could add an additional 10% to the uncertainty range. Propagating this additional 10% uncertainty gives $k_{20} = (5.7 \pm 0.7) \times 10^{-12}$ and $(6.2 \pm 0.7) \times 10^{-12}$ cm$^3$ molecule$^{-1}$ s$^{-1}$. We choose to report the average of these two determinations with error limits encompassing the extremes of the determinations. Hence, $k_{20} = (6.0 \pm 1.0) \times 10^{-12}$ cm$^3$ molecule$^{-1}$ s$^{-1}$. This result is in excellent agreement with the value of $k_{20} = 6.1 \times 10^{-12}$ cm$^3$ molecule$^{-1}$ s$^{-1}$ reported in the absolute rate study of Zabarnick et al.[20]

**3.9. Kinetics of the Reaction of Cl Atoms with 1,3,5-Trioxane and Methylene Glycol Diformate.** Prior to investigating the atmospheric fate of (c-$C_3H_5O_3$)O(•) radicals, relative rate experiments were performed using the FTIR systems to investigate the kinetics of the reactions of Cl atoms with 1,3,5-trioxane and HC(O)$OCH_2$OC(O)H (an oxidation product of 1,3,5-trioxane). Photolysis of molecular chlorine was used as a source of Cl atoms.

$$Cl_2 \xrightarrow{h\nu} 2\ Cl \qquad (23)$$

$$Cl + \text{(c-C3H5O3)} \longrightarrow \text{products} \qquad (24)$$

$$Cl + HC(O)OCH_2OC(O)H \longrightarrow \text{products} \qquad (25)$$

The kinetics of reaction 24 were measured relative to reactions 26−28 while reaction 25 was measured relative to (29) and (30). HC(O)$OCH_2$OC(O)H was prepared in situ by the UV irradiation of mixtures of 10−11 mTorr of methoxymethyl formate ($CH_3OCH_2OC(O)H$) and 150 mTorr of $Cl_2$ in 700 Torr of $O_2$. The resulting HC(O)$OCH_2$OC(O)H was readily identified by its characteristic IR features at 955, 1091, 1169 and 1769 cm$^{-1}$.[21] The increase of HC(O)$OCH_2$OC(O)H was directly proportional

$$Cl + C_2H_4 \longrightarrow \text{products} \qquad (26)$$

$$Cl + CH_3OCH_3 \longrightarrow \text{products} \qquad (27)$$

$$Cl + CH_3OH \longrightarrow \text{products} \qquad (28)$$

$$Cl + CH_4 \longrightarrow \text{products} \qquad (29)$$

$$Cl + CH_3Cl \longrightarrow \text{products} \qquad (30)$$

to the loss of methoxymethyl formate for all ranges of consumption showing that the reactivity of Cl atoms toward methoxymethyl formate is much greater than that toward HC(O)$OCH_2$OC(O)H. When the methoxymethyl formate had been totally consumed, small amounts (15 mTorr) of a reference compound ($CH_4$ or $CH_3Cl$) were added. The irradiation was continued, and the decay of HC(O)$OCH_2$OC(O)H and reference was monitored.

The observed loss of 1,3,5-trioxane and HC(O)$OCH_2$OC(O)H versus those of the reference compounds is shown in Figure 9. In the 1,3,5-trioxane experiments 700 Torr of $N_2$ or air diluent was used; there was no discernible effect of the diluent gas on the results. Linear least-squares analysis on the data in Figure 9 gives $k_{24}/k_{26} = 1.08 \pm 0.06$, $k_{24}/k_{27} = 0.59 \pm 0.03$, $k_{24}/k_{28} = 1.77 \pm 0.10$, $k_{25}/k_{29} = 5.4 \pm 0.5$, and $k_{25}/k_{30} = 1.01 \pm 0.12$. Using $k_{26} = 9.4 \times 10^{-11}$,[22] $k_{27} = 1.9 \times 10^{-10}$,[23] $k_{28} = 5.4 \times 10^{-11}$,[22] $k_{29} = 1.0 \times 10^{-13}$,[22] and $k_{30} = 4.8 \times 10^{-13}$ [22] gives $k_{24} = (1.02 \pm 0.06) \times 10^{-10}$, $k_{24} = (1.12 \pm 0.06) \times 10^{-10}$, $k_{24} = (9.6 \pm 0.5) \times 10^{-11}$, $k_{25} = (5.4 \pm 0.5) \times 10^{-13}$, and $k_{25} = (4.8 \pm 0.6) \times 10^{-13}$ cm$^3$ molecule$^{-1}$s$^{-1}$. Consistent results were obtained using the different reference compounds. We choose to quote values for $k_{24}$ and $k_{25}$ which are the averages of the results above with error limits which encompass the extremes of the ranges; hence, $k_{24} = (1.03 \pm 0.15) \times 10^{-10}$ and $k_{25} = (5.1 \pm 0.9) \times 10^{-13}$ cm$^3$ molecule$^{-1}$ s$^{-1}$. We estimate that potential systematic errors associated with uncertainties in the reference rate constants could add an additional 10% to the uncertainty range. Propagating this additional uncertainty gives $k_{24} = (1.03 \pm 0.18) \times 10^{-10}$ and $k_{25} = (5.1 \pm 1.0) \times 10^{-13}$ cm$^3$ molecule$^{-1}$ s$^{-1}$. There are no literature data to compare with these results.

**3.10. FTIR Study of the Atmospheric Fate of the Alkoxy Radical (c-$C_3H_5O_3$)O(•).** To determine the atmospheric fate of the alkoxy radical (c-$C_3H_5O_3$)O(•) formed from reaction 6a, the FTIR−smog chamber systems were used to study the products resulting from the Cl atom initiated oxidation of 1,3,5-trioxane in the presence of NO. All experiments were performed in 700−750 Torr total pressure of $N_2/O_2$ diluent at 296 K. The aim of these experiments was to determine the relative importance of reactions 31 and 32 in the atmospheric chemistry of (c-$C_3H_5O_3$)O(•) radicals.

$$\text{(c-C3H5O3)O(•)} + M \longrightarrow H(O)COCH_2OCH_2O(\cdot) + M \qquad (31)$$

$$\text{(c-C3H5O3)O(•)} + O_2 \longrightarrow \text{(c-C3H5O4)} + HO_2 \qquad (32)$$

The loss of 1,3,5-trioxane and the formation of products were monitored using FTIR spectroscopy. Figure 10 shows IR spectra acquired before (A) and after (B) a 30 s irradiation of a mixture of 8.0 mTorr of 1,3,5-trioxane, 87 mTorr of $Cl_2$, 12 mTorr of NO, and 592 Torr of $O_2$ in 700 Torr total pressure of $N_2$ diluent. Subtraction of features attributable to 1,3,5-trioxane, NO, $NO_2$, ClNO, $ClNO_2$, HONO, $HONO_2$, and $HO_2NO_2$ from panel B gives the infrared product features shown in panel C. By comparison with the available literature spectrum,[21] we

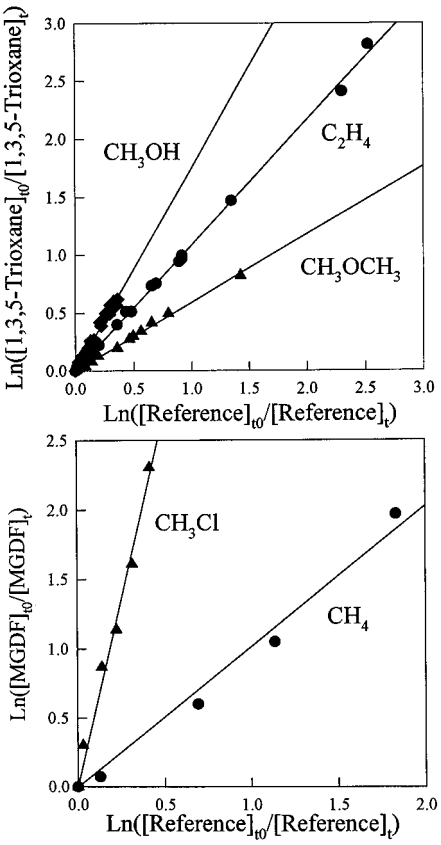


**Figure 9.** Decay of 1,3,5-trioxane versus $CH_3OH$, $C_2H_4$, and $CH_3OCH_3$ (top) and methylene glycol diformate (MGDF) versus $CH_3Cl$ and $CH_4$ (bottom) when mixtures of these compounds were exposed to Cl atoms in 700−750 Torr total pressure at 295 K.

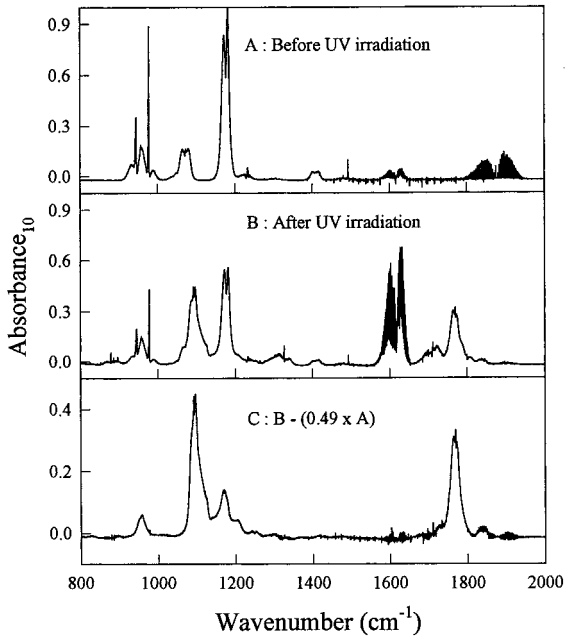


**Figure 10.** IR spectra acquired before (A) and after (B) a 30 s irradiation of a mixture of 8.0 mTorr of 1,3,5-trioxane, 87 mTorr of $Cl_2$, 12 mTorr of NO, and 592 Torr of $O_2$ in 700 Torr total pressure of $N_2$ diluent. During the irradiation 51% of the 1,3,5-trioxane was consumed. Subtraction of features attributable to 1,3,5-trioxane, NO, $NO_2$, ClNO, $ClNO_2$, HONO, $HONO_2$, and $HO_2NO_2$ from panel B gives panel C. We assign the IR features at 957, 1091, 1168, and 1769 cm$^{-1}$ in panel C to methylene glycol diformate, $H(O)COCH_2OC(O)H$.

assign the IR features at 955, 1091, 1169, and 1769 cm$^{-1}$ in panel C to methylene glycol diformate, $H(O)COCH_2OC(O)H$.

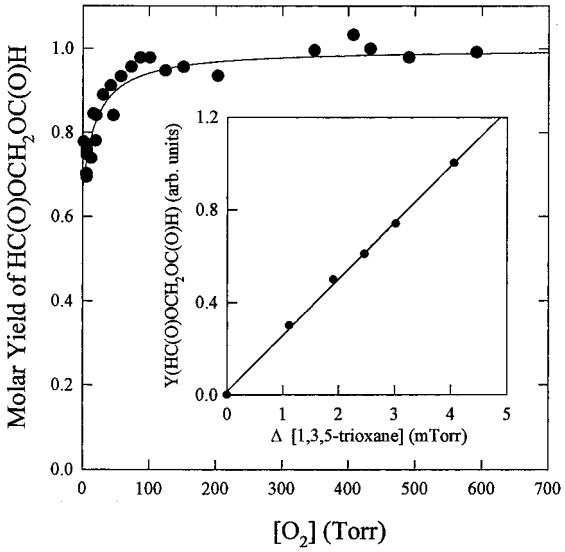


**Figure 11.** Yield of methylene glycol diformate following the UV irradiation of 1,3,5-trioxane/$Cl_2$/NO/$O_2$/$N_2$ mixtures as a function of the $O_2$ partial pressure at constant total pressure (700 or 750 Torr) and 296 ± 2K. The curve through the data is a fit; see text for details. The insert shows the formation of methylene glycol diformate versus loss of 1,3,5-trioxane for an experiment employing 8.0 mTorr of 1,3,5-trioxane, 87 mTorr of $Cl_2$, 12 mTorr of NO, and 592 Torr of $O_2$, at 700 Torr total pressure with $N_2$ diluent.

As shown in the insert in Figure 11, the concentration of methylene glycol diformate increased linearly with the loss of 1,3,5-trioxane over the range of 1,3,5-trioxane consumptions used in the present work (8−85%). Methylene glycol diformate is formed via reaction 31 followed by either reaction 33, or reaction 34, or both.

$$H(O)COCH_2OCH_2O(\cdot) + O_2 \longrightarrow H(O)COCH_2OC(O)H + HO_2 \quad (33)$$

$$H(O)COCH_2OCH_2O(\cdot) + M \longrightarrow H(O)COCH_2OC(O)H + H + M \quad (34)$$

To confirm the identification of methylene glycol diformate, mixtures of methoxymethyl formate ($CH_3OCH_2OCHO$) and $Cl_2$ in 700 Torr of $O_2$ were subject to UV irradiation. The resulting product spectra had IR features at 957, 1091, 1168, and 1769 cm$^{-1}$ which matched those observed in the 1,3,5-trioxane experiments. It is expected that a substantial fraction of the reaction of Cl atoms with $CH_3OCH_2OCHO$ occurs at the $CH_3$− group resulting in the oxidation of $CH_3OCH_2OCHO$ to methylene glycol diformate. The coincidence of the IR product features provides confirmation of our identification of methylene glycol diformate.

In experiments using the 1080 L quartz glass reactor and super actinic fluorescent lamps, distinct curvature was observed in plots of the concentration of methylene glycol diformate as a function of the loss of 1,3,5-trioxane. This curvature was not observed for experiments performed in the 405 L Pyrex reactor equipped with the same UV light source. Tests indicate that the curvature is primarily due to photolysis of methylene glycol diformate with a photolysis frequency of between $10^{-3}$ and $10^{-4}$ s$^{-1}$. Under the assumption of a quantum yield of 1 for the photolysis, extrapolation of the chamber results to atmospheric conditions[24] suggests upper limits for the photolysis frequency of methylene glycol diformate between $J = 3 \times 10^{-3}$ and $0.3 \times 10^{-3}$ s$^{-1}$ for July 1 clear sky conditions at a latitude of 40° N corresponding to an atmospheric photolysis lifetime of between 6 and 57 min.

Product features at 1640−1680 cm$^{-1}$ characteristic of alkyl nitrates were searched for but were not found suggesting that

reaction 6 proceeds predominately, if not exclusively, via channel (6a).

To investigate the dependence of the methylene glycol diformate yield on the $O_2$, partial pressure experiments were performed using mixtures of 6−14 mTorr of 1,3,5-trioxane, 10−100 mTorr $Cl_2$, 5−20 mTorr NO, and 2.1−592 Torr $O_2$, in 700−750 Torr total pressure of $N_2$ diluent. Methylene glycol diformate was observed as a major product in all experiments. As seen in Figure 11, for experiments employing $[O_2] = 100-600$ Torr there was no discernible effect of $[O_2]$ on the yield of methylene glycol diformate.

Unfortunately, we do not have a sample of methylene glycol diformate and so we cannot calibrate its IR features. In light of the absence of any other IR product features it seems reasonable to assume that reaction 6 proceeds essentially 100% via channel (6a) and that in the presence of >300 Torr of $O_2$ the subsequent conversion of the alkoxy radical (c-$C_3H_5O_3$)O(•) into methylene glycol diformate is 100% effective. These assumptions were used to derive the absolute scale of the *y*-axis in Figure 11.

As shown in Figure 11, for experiments employing $[O_2] <$ 50 Torr the observed yield of methylene glycol diformate was significantly less than in experiments with $[O_2] >$ 100 Torr. The fact that the yield of methylene glycol diformate drops when $[O_2]$ is decreased below 50 Torr shows that additional loss mechanisms become important for the alkoxy radical HC(O)$OCH_2OCH_2O$(•) formed in reaction 31. It is conceivable that reaction with $Cl_2$ and/or NO compete with $O_2$ for the available $HC(O)OCH_2OCH_2O$(•) radicals. To test for the effect of [NO] and $[Cl_2]$ on the observed product yields, experiments were performed with $[O_2] = 6$ Torr and [NO] and $[Cl_2]$ varied independently over the ranges 5−18 and 31−89 mTorr, respectively. While there was no observable effect of $[Cl_2]$ over the range stated, increasing [NO] from 5 to 18 mTorr resulted in small (≈10%) but significant decrease in the methylene glycol diformate yield. Presumably this small decrease reflects scavenging of $HC(O)OCH_2OCH_2O$(•) radicals via reaction with NO to give the nitrite $HC(O)OCH_2OCH_2ONO$. To minimize complications caused by such an effect, only data obtained using [NO] < 10 mTorr are shown in Figure 11.

As seen from Figure 11, the yield of methylene glycol diformate, while sensitive to the $O_2$ partial pressure, does not approach zero at the lowest $O_2$ pressures studied. Such behavior suggests that there are two pathways by which methylene glycol diformate is formed in the chamber; one pathway is dependent upon $O_2$, and the other is not. The trend of the data shown in Figure 11 suggests that there are at least three competing fates for the $HC(O)OCH_2OCH_2O$(•) radicals:

$$H(O)COCH_2OCH_2O(\cdot) + O_2 \longrightarrow H(O)COCH_2OC(O)H + HO_2 \quad (33)$$

$$H(O)COCH_2OCH_2O(\cdot) + M \longrightarrow H(O)COCH_2OC(O)H + H + M \quad (34)$$

$$H(O)COCH_2OCH_2O(\cdot) \longrightarrow \text{other products} \quad (35)$$

The expected dependence of the yield of methylene glycol diformate on the $O_2$ partial pressure can be expressed as:

$$Y(H(O)COCH_2OC(O)H) = \left( \frac{\left(\frac{k_{33}}{k_{34}}\right)[O_2] + 1}{\left(\frac{k_{33}}{k_{34}}\right)[O_2] + 1 + \left(\frac{k_{33}}{k_{34}}\right)} \right)$$

The above expression was fitted to the data in Figure 11 with two parameters varied simultaneously, $k_{33}/k_{34}$ and $k_{35}/k_{34}$. Best fit values of $k_{33}/k_{34} = 0.07 \pm 0.04$ Torr$^{-1}$ and $k_{35}/k_{34} = 0.5 \pm 0.2$ were obtained. Using these results it can be calculated that in the presence of 1 atm of air diluent ($[O_2] = 160$ Torr) the yield of methylene glycol diformate will be 96%.

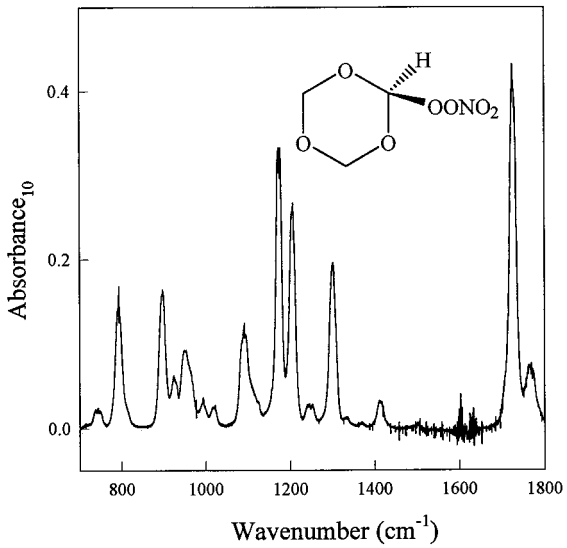


**Figure 12.** IR spectrum of 3.9 mTorr of the peroxy nitrate (c-$C_3H_5O_3$)$O_2NO_2$. The IR path length was 28 m.

Thus far, we have not addressed the products of reaction 35. In addition to reactions 33 and 34, possible fates of H(O)$COCH_2OCH_2O$(•) radicals include decomposition and isomerization via internal H-atom abstraction. Eberhard et al.[25] and Atkinson and Aschmann[26] have shown that isomerization is important for aliphatic $C_6$ and $C_7$ alkoxy radicals. The analysis presented above is unaffected by the exact mechanism of the reaction 35. For experiments conducted with low $O_2$ partial pressures, IR features attributed to one or more unknown products were observed at 757, 915, 1033, 1070, 1124, and 1195 cm$^{-1}$, which are presumably attributable to products following isomerization and/or decomposition of the $H(O)COCH_2OCH_2O$(•) radicals.

Finally, we need to consider how our results fit in with the available data concerning the atmospheric degradation mechanisms of other alkoxy radicals. The results from the present work show that under atmospheric conditions at least three loss mechanisms compete for $H(O)COCH_2OCH_2O$(•) radicals. Similar conclusions were reached in recent studies of the alkoxy radicals derived from dimethyl carbonate, $CH_3OC(O)OCH_2O$(•)[5] and dimethoxymethane $CH_3OCH_2OCH_2O$(•).[18] There are obvious structural similarities between these alkoxy radicals, and similar behavior is reasonable.

**3.11. IR Spectrum and Thermal Decomposition Rate of the Peroxy Nitrate Derived from 1,3,5-Trioxane.** The UV irradiation of 1,3,5-trioxane/$Cl_2$/NO/$O_2$/$N_2$ mixtures resulted in consumption of NO and formation of methylene glycol diformate and $NO_2$. When all of the NO had been consumed, additional product features at 792, 897, 923, 949, 1090, 1174, 1206, 1301, 1412, 1726, and 1769 cm$^{-1}$ were observed. The same IR product features were observed following irradiation of 1,3,5-trioxane/$Cl_2$/$NO_2$/$O_2$ mixtures. These features increased linearly with the consumption of 1,3,5-trioxane and are ascribed to the formation of the peroxy nitrate (c-$C_3H_5O_3$)$O_2NO_2$ via reaction 7.

The IR spectrum of the peroxy nitrate, (c-$C_3H_5O_3$)$O_2NO_2$, is shown in Figure 12. There was no discernible loss (<2%) of (c-$C_3H_5O_3$)$O_2NO_2$ on standing in the dark in the chamber for 10 min. However, addition of NO resulted in a complete (>95%) loss of (c-$C_3H_5O_3$)$O_2NO_2$ within the 2 min taken for

the addition. As with other alkyl peroxy nitrates, (c-$C_3H_5O_3$)$O_2$-$NO_2$ is thermally unstable and decomposes to give (c-$C_3H_5O_3$)-$O_2$(•) radicals and $NO_2$. In the presence of $NO_2$ the peroxy nitrate is re-formed via reaction 7. Addition of NO serves to scavenge the (c-$C_3H_5O_3$)$O_2$(•) radicals and prevents the re-formation of the peroxy nitrate. The thermal stability of the peroxy nitrate derived from 1,3,5-trioxane is low, and like other alkyl peroxy nitrates,[16] it will not play any role in atmospheric chemistry.

## 4. Discussion

A substantial body of kinetic and mechanistic data pertaining to the atmospheric chemistry of 1,3,5-trioxane are presented here. It is expected that the atmospheric lifetime of 1,3,5-trioxane is determined by reaction with OH radicals. While the OH radical concentration in the atmosphere varies with location, time of day, season, and meteorological conditions, a reasonable 24 h global average is $(0.5-1.0) \times 10^6$ cm$^{-3}$.[27-29] At 296 K, the rate constant for reaction of OH radicals with 1,3,5-trioxane is $6.0 \times 10^{-12}$ cm$^3$ molecule$^{-1}$ s$^{-1}$; hence, the atmospheric lifetime of 1,3,5-trioxane will be 2−4 days. Reaction with OH will produce an alkyl radical which will add $O_2$ rapidly (within 1 $\mu$s) to give a peroxy radical. In polluted urban air masses the peroxy radical will react with NO within a few minutes which leads to the formation of methylene glycol diformate. As with other formates, methylene glycol diformate is expected to be relatively unreactive toward OH radicals and is not expected to participate in further gas-phase reactions in urban airsheds. As discussed in section 3.10, there is evidence from the present work that methylene glycol diformate may undergo rapid photolysis in the sunlit troposphere. It is interesting to contrast this preliminary conclusion with the recent work by Vésine and Mellouki[30] which shows that monoformates (methyl, ethyl, propyl, and butyl formate) do not absorb at wavelengths greater than 260 nm and hence do not undergo photolysis in the lower atmosphere. Clearly, additional studies are needed to clarify the atmospheric fate of methylene glycol diformate.

It is interesting to note that the atmospheric fate of the alkoxy radical derived from 1,3,5-trioxane, (c-$C_3H_5O_3$)O(•), is decomposition via C−O bond scission. It has been reported previously that alkoxy radicals derived from ethers undergo decomposition via C−C bond scission, H-atom elimination, or reaction with $O_2$. The alkoxy radical derived from 1,3,5-trioxane is the first example of an alkoxy radical in which C−O bond scission is important. The behavior of the (c-$C_3H_5O_3$)O(•) can be compared with that of the structurally similar $CH_3OCH$-(O•)$OCH_3$ derived from dimethoxymethane. The sole atmospheric fate of $CH_3OCH$(O•)$OCH_3$ radicals is reaction with $O_2$ to give $CH_3OC$(O)$OCH_3$ (dimethyl carbonate).[5] That there is no evidence of a similar reaction of (c-$C_3H_5O_3$)O(•) radicals with $O_2$ presumably reflects the ring strain involved in formation of the cyclic carbonate. Further research is needed to elucidate the factors which influence the atmospheric fate of alkoxy radicals.

**Acknowledgment.** Financial support of the work conducted at the Bergische Universität Wuppertal by the European Commission and the Bundesminister für Bildung, Forschung und Technologie (BMBF) is gratefully acknowledged. The work at Risø was supported by the European Commission and the Ford Forschungzentrum, Aachen, Germany.

## References and Notes

(1) Roubi, M. A. *Chem. Eng.* **1995**, *44*, 37.
(2) Hansen, K. B.; Wilbrandt, R.; Pagsberg, P. *Rev. Sci. Instr.* **1979**, *50*, 1532.
(3) Sehested, J. Ris¢-R-804, 1994.
(4) Wallington, T. J.; Japar, S. M. *J. Atmos. Chem.* **1989**, *9*, 399.
(5) Bilde, M.; Møgelberg, T. E.; Sehested, J.; Nielsen, O. J.; Wallington, T. J.; Hurley, M. D.; Japar, S. M.; Dill, M.; Orkin, V. L.; Buckley, T. J.; Huie, R. E.; Kurylo, M. J. *J. Phys. Chem. A* **1997**, *101*, 3514.
(6) Wallington, T. J.; Dagaut, P.; Kurylo, M. J. *Chem. Rev.* **1992**, *92*, 667.
(7) Barnes, I.; Becker, K. H.; Fink, E. H.; Reimer, A.; Zabel, F.; Niki, H. *Int. J. Chem. Kinet*. **1983**, *15*, 631.
(8) Barnes, I.; Becker, K. H.; Mihalopoulos, N. *J. Atmos. Chem*. **1994**, *18*, 267.
(9) Wallington, T. J.; Japar, S. M. *J. Atmos. Chem.* **1989**, *9*, 399.
(10) Wallington, T. J.; Hurley, M. D.; Shi, J.; Maricq, M. M.; Sehested, J.; Nielsen, O. J.; Ellermann, T. *Int. J. Chem. Kinet.* **1993**, *25*, 651.
(11) Platz, J. Unpublished data obtained at Risø National Laboratory.
(12) Platz, J.; Sehested, J.; Møgelberg, T. E.; Nielsen, O. J.; Wallington, T. J. *J. Chem. Soc., Faraday Trans.* **1997**, *93*, 2855.
(13) Mallard, W. G.; Westley, F.; Herron, J. T.; Hampson, R. F. *NIST Chemical Kinetics Database*, Ver 6. 0; NIST Standard Reference Data; NIST: Gaithersburg, MD, 1994.
(14) Ellermann, T.; Sehested, J.; Nielsen, O. J.; Pagsberg, P.; Wallington, T. J. *Chem. Phys. Lett.* **1994**, *218*, 287.
(15) Maricq, M. M.; Szente, J. J. *J. Phys. Chem.* **1992**, *96*, 4925.
(16) . Lightfoot, P. D.; Cox, R. A.; Crowley, J. N.; Destriau, M.; Hayman, G. D.; Jenkin, M. E.; Moortgat, G. K.; Zabel, F. *Atmos. Environ.* **1992**, *26*, 1805.
(17) Sehested, J.; Nielsen, O. J.; Wallington, T. J. *Chem. Phys. Lett.* **1993**, *213*, 257.
(18) Wallington, T. J.; Hurley, M. D.; Ball, J. C.; Straccia, A. M.; Platz, J.; Christensen, L. K.; Sehested, J.; Nielsen, O. J. *J. Phys. Chem. A* **1997**, *101*, 5302.
(19) Atkinson, R. *J. Phys. Chem. Ref. Data* **1994**, *Monograph 2*.
(20) Zabarnick S.; Fleming, J. W.; Lin, M. C. *Int. J. Chem. Kinet*. **1988**, *20*, 117.
(21) Schaap, A. P. *Tetrahedron Lett.* **1971**, *21*, 1757.
(22) DeMore, W. B.; Sander, S. P.; Golden, D. M.; Hampson, R. F.; Kurylo, M. J.; Howard, C. J.; Ravishankara, A. R.; Kolb, C. E.; Molina, M. J. *Publication 97-4*; Jet Propulsion Laboratory: Pasadena, CA, 1997.
(23) Langer, S.; Ljungström, E.; Wängberg, I.; Wallington, T. J.; Hurley, M. D.; Nielsen, O. J. *Int. J. Chem. Kinet.* **1996**, *28*, 299.
(24) Klotz, B.; Barnes, I.; Becker, K. H.; Golding, B. T. *J. Chem. Soc., Faraday Trans.* **1997**, *93*, 1507.
(25) Eberhard, J.; Müller, C.; Stocker, D. W.; Kerr, J. A. *Environ. Sci. Technol*. **1995**, *29*, 232.
(26) Atkinson, R.; Aschmann, S. M. *Int. J. Chem. Kinet*. **1995**, *27*, 261.
(27) Ravishankara, A. R.; Lovejoy, E. R. *J. Chem. Soc., Faraday Trans.* **1994**, 90, 2159.
(28) Dorn, H.-P.; Brandenburger, U.; Brauers, T.; Ehhalt, D. H. *Geophys. Res. Lett*. **1996**, *23*, 2537.
(29) Hofzumahaus, A.; Aschmutat, U.; Hessling, M.; Holland, F.; Ehhalt, D. H. *Geophys. Res. Lett.* **1996**, *23*, 2541.
(30) .Vésine, E.; Mellouki, A. *J. Chim. Phys. Phys.-Chim. Biol*. **1997**, *94*, 1634.